Plate Motions Around the Red Sea Since the Early Oligocene

Antonio Schettino, Chiara Macchiavelli, and Najeeb M. A. Rasul

Abstract

The Red Sea represents a very young oceanic basin that formed between Nubia and Arabia since chron C3 (~4.6 Ma). The rifting phase started at ~30 Ma (early Oligocene) and can be represented by two kinematic stages, characterized by distinct directions of extension and different duration. Deformation associated with rifting was accommodated through the reactivation of the inherited Proterozoic structures. We show that the first stage was characterized by the northward motion of the Arabian plate with respect to Africa, accompanied by a pattern of deformation that included N–S oriented strike–slip faults and normal faults having E–W strike. During this stage, extension was mainly accommodated by the formation of pull–apart basins. Starting from ~27 Ma (late Oligocene), the extension axes changed dramatically and acquired the modern NE–SW pattern, which was conserved until the early Pliocene in the southern Red Sea and is still active in the northern region. In this time interval, an inherited system of NW–SE structures was reactivated as normal faults accommodating NE–SW extension, while NE–SW Proterozoic structures were reactivated as transfer strike–slip faults. Although no changes in the directions of extension are observed during this interval, two significant tectonic events occurred around 14 Ma and at 1.77 Ma. During the Langhian, two intervening microplates formed between Nubia and Arabia; the Danakil and Sinai microplates, whose motion determined the formation of the Afar Depression and the Gulf of Aqaba, respectively. Finally, starting from the Pleistocene, ongoing collision of Arabia with Eurasia along the Zagros mountains resulted into a dramatic slowdown in the Red Sea opening rates.

A. Schettino (✉)
School of Science and Technology – Geology Division, University of Camerino, Via Gentile III Da Varano, 62032 Camerino, MC, Italy
e-mail: antonio.schettino@unicam.it

C. Macchiavelli
Institute of Earth Sciences Jaume Almera, ICTJA-CSIC, Lluis Sole I Sabaris S/N, 08028 Barcelona, Spain

N. M. A. Rasul
Center for Marine Geology, Saudi Geological Survey, Jeddah, Saudi Arabia

N. M. A. Rasul and I. C. F. Stewart (eds.), *Geological Setting, Palaeoenvironment and Archaeology of the Red Sea*,
https://doi.org/10.1007/978-3-319-99408-6_9

1 Introduction

Determining the kinematics of the tectonic plates surrounding the Red Sea and the Gulf of Aden (Fig. 1) represents a fundamental step toward a comprehension of the fundamental geodynamic processes driving the formation of new tectonic plates. The rifting and spreading history of the Gulf of Aden has been described accurately during the past few years by the analysis of marine magnetic anomalies, fracture zones, and seismic profiles (e.g., d'Acremont et al. 2005; Fournier et al. 2010; Leroy et al. 2010). In the case of the Red Sea, a similar approach has recently led to the characterization of the spreading kinematics during the last ~4.6 Ma (Schettino et al. 2016). However, a quantitative description of the Nubia–Arabia kinematics during the rifting phase is still controversial and several alternative solutions have been proposed so far, with regard to the age of initiation of rifting, the age of rift–drift transition, the width of the thinned continental margins, and the amount and directions of extension.

McKenzie et al. (1970) were the first to propose a reconstruction of the relative positions of Arabia and Nubia during the Miocene, based on a best–fitting procedure of coastline segments north of 15°N and the assumption that most of the Red Sea was floored by oceanic crust. These authors mentioned some evidence that the Euler pole of rotation between these plates had remained constant during the opening of the Red Sea and inferred an age of 15 Ma for the initiation of this process, assuming that a steady spreading rate of 10 mm yr^{-1} was maintained and that neither Africa nor Arabia deformed significantly during the

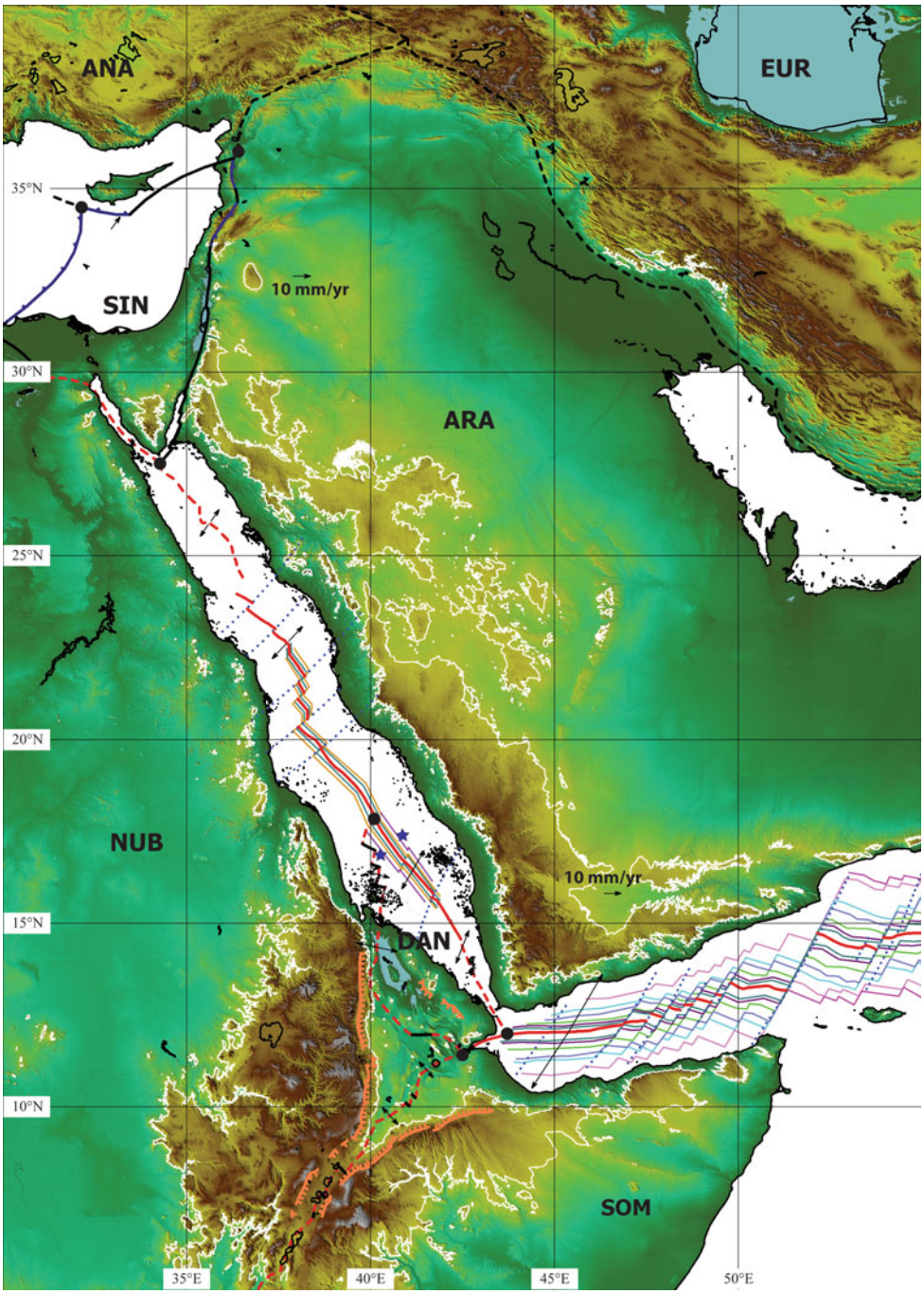

Fig. 1 Location map, showing present-day plate boundaries, velocity fields, triple junctions, magnetic isochrons, and fracture zones around the Red Sea and Gulf of Aden (from Schettino et al. 2016 and Fournier et al. 2010). Red solid lines: Mid-ocean ridges; Red dashed lines: Rift axes; Blue dotted lines: Fracture zones; Black solid lines: Strike-slip faults; Blue lines with barbs: Convergent boundaries; Black dashed lines: Plate boundaries outside the study area; White line: 1000 m topography contour; Orange lines with barbs: Main rift shoulders; Black dots: Triple junctions; Stars in the southern Red Sea indicate the locations where the oldest oceanic crust (4.62 Ma, early Pliocene) has been identified; Magnetic isochrons 2, 2A, and 3 in the Red Sea are shown in green, ochre, and purple, respectively; ANA = Anatolia, EUR = Eurasia, SIN = Sinai, ARA = Arabia, NUB = Nubia, DAN = Danakil, SOM = Somalia. Areas in blue are continental inland below sea level. Fracture zones in the Gulf of Aden are from Leroy et al. (2012). Magnetic isochrons in the Gulf of Aden are: 2Ay, 2Ao, 3A, 4A, 5, 5C, 5D, and 6 (after Fournier et al. 2010)

rifting stage (i.e., the amount of extension of the margins was assumed to be nearly zero, so that $\beta \approx 1$). A thorough discussion of the discrepancies between such a rigid plates approximation and geological observations can be found in Le Pichon and Francheteau (1978). In addition, these authors showed that models based on the assumption that the whole Red Sea is floored by Oligocene to recent oceanic crust extending from coast to coast are not compatible with simple geodynamic considerations. Some years later, Cochran (1983) provided the first estimate of stretching for the conjugate continental margins of Arabia and Nubia in the northern Red Sea, about 160 km at 25°N ($\beta = 1.3$). However, a much higher amount of extension, with β ranging from 3.45 to 2.6, was proposed by Joffe and Garfunkel (1987) for the area north of ~17°N.

Regarding the age of initiation of sea floor spreading, while there is now general agreement that it was Chron C6n (~20.1 Ma, early Burdigalian) in the eastern Gulf of Aden (Fournier et al. 2010), the timing is still controversial in the case of the Red Sea. In fact, it depends on the different

interpretations given to the nature of the crust below the up to 5 km thick layer of Miocene evaporites overlying the basement. For example, Le Pichon and Gaulier (1988) assumed that the Red Sea crust is oceanic even in the northernmost area, up to 26.3°N, from the axial zone up to a distance of about 35 km from the coastlines. Accordingly, they estimated that sea floor spreading would have initiated at ~13 Ma if the spreading rate remained constant. In general, in the model of Le Pichon and Gaulier (1988) rifting started at ~30 Ma and proceeded as a slow rotation (~0.06°/Myr) about a constant Euler pole up to ~13 Ma. Then, starting from this age the rotation of Arabia relative to Nubia was accompanied by sea floor spreading at a rate of ~0.42°/Myr about the same Euler pole. More recent GPS estimates have suggested an early Miocene (~24 Ma) age of initiation of rifting in both the Red Sea and the Gulf of Aden (ArRajehi et al. 2010), with a 70% increase in the angular velocity of separation between Nubia and Arabia at 13 Ma without changes in the stage pole location. This kinematic model is partially retained in the very recent work of DeMets and Merkouriev (2016), although these authors propose a three-stages tectonic evolution of the Red Sea, such that two early stages before Chron C5C (~16 Ma) have stage poles slightly different from the pole of rotation of ArRajehi et al. (2010).

In this paper, we estimate the amount of syn-rift extension around the Red Sea on the basis of a palinspastic restoration of the stretched margins to their pre-rift width. To this purpose, we will compile a Moho grid for the Red Sea region, which will be combined with Aster GDEM topography to analyse a series of crustal cross-sections across the Red Sea using the method illustrated in Schettino (2014). Then, taking into account that no change in the directions of extension has been observed along the conjugate margins (e.g., Schettino et al. 2016), the resulting finite strain can be used to determine the angular syn-rift separation between Arabia and Nubia.

2 Recent Kinematics of the Red Sea

A quantitative determination of the sea-floor spreading history of an oceanic basin requires the identification of magnetic anomaly crossings, transform faults, and fracture zone trends. The first comprehensive analysis of sea-floor spreading anomalies in the Red Sea was performed by Chu and Gordon (1998), who did not include transform fault offsets in their study because of the short offset of these features, which never exceeds 5 km in the southern Red Sea. More recently, we have shown that a set of transverse structures exists in the Red Sea region, whose formation is associated with the progressive oceanization of the conjugate margins. Schettino et al. (2016) argued that these features have a strike that is representative of the directions of relative motion during the latest rifting stage and onset of sea floor spreading. Therefore, these authors combined both directional data and sea-floor spreading anomalies to build a refined kinematic model since 4.6 Ma, which is the age of the oldest oceanic crust identified in the southern Red Sea around 17.1°N (Fig. 1). The magnetic isochrons of this new model are shown in Fig. 1. The model describes the five-plates system formed by Nubia, Arabia, Somalia, and the Sinai and Danakil microplates. The predicted flow lines of relative motion are illustrated in Fig. 2. These lines determine the local azimuth of relative motion between any plate pair. The trends in Fig. 2 show that Danakil is separating from Arabia by anti-clockwise rotation about a pole located in the Gulf of Aden, whereby the velocity of separation between the two plates decreases southward. Consequently, rifting of Danakil from Arabia occurred with strain rates higher in the northern part of the southern Red Sea. Actually, the southern part of this region from 14.8°N up to the Bab al Mandeb area is still in the rifting stage. Figure 2 also shows that Danakil is rifting from Nubia with extension directions that vary from E–W in southern Afar to NW–SE close to the triple junction. Figure 2 also illustrates the pattern of relative motions in the northernmost Red Sea. In the model of Schettino et al. (2016), Sinai is an independent microplate that is separating from Nubia through a trans-tensional boundary in the Gulf of Suez while sliding apart with respect to Arabia through the transcurrent Dead Sea Fault Zone (DSFZ). Finally, as shown in Figs. 1 and 2, the northern Red Sea at latitudes higher than 24°N is still in the rifting stage. A very young spreading ridge, which is not yet flanked by magnetic isochrons, can be found north of 22.6°N. This ridge is formed by three spreading segments separated by two transform faults, whose landward continuations form two major active transverse structures.

3 Plate Reconstructions for the Late Langhian—Early Pliocene Time Interval

A set of plate reconstructions at anomalies 3n.2r (4.62 Ma), 3n (4.18 Ma), 2A (2.58 Ma), and 2 (1.77 Ma), illustrating the plate tectonic evolution of the Red Sea since the early Pliocene, has been presented by Schettino et al. (2016). In this study, the starting point is represented by the oldest of these reconstructions, namely by the early Pliocene configuration (4.62 Ma), which will be extrapolated backward to reconstruct the most recent stage of rifting in the Red Sea. As mentioned above, the early Pliocene represents the age of the oldest oceanic crust identified in the Red Sea. Figure 3a and b show plate boundaries and velocity fields during this time interval. There is strong geological and structural evidence that this configuration of the plate boundaries is representative of a tectonic phase that started in the middle Miocene

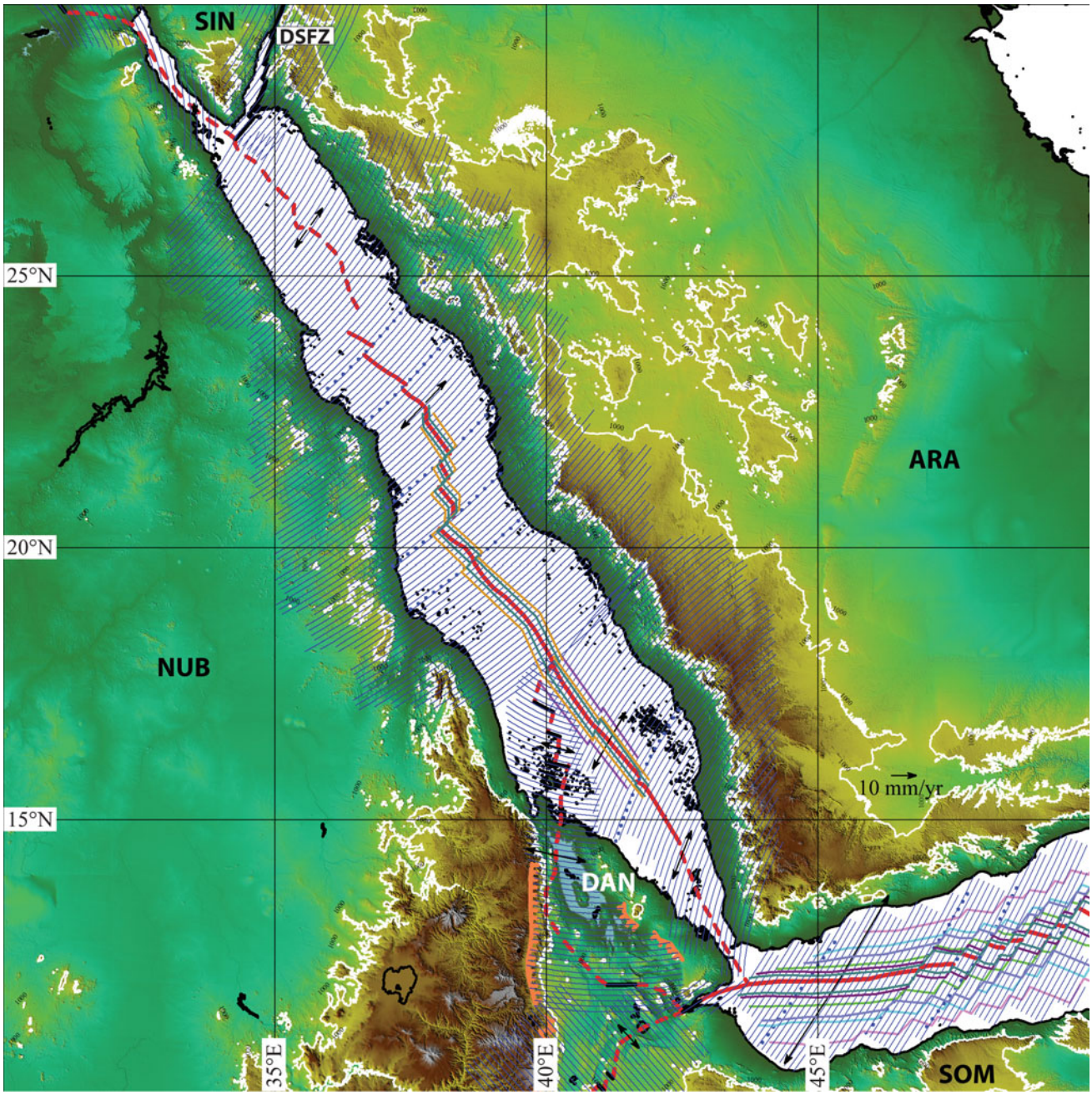

Fig. 2 Flow lines and relative velocity field of current plate motions in the Red Sea and in the Gulf of Aden. Local relative velocity between two plates along a boundary region or a deformation zone is always tangent to these lines. DSFZ = Dead Sea Fault Zone. (From Schettino et al. 2016, their Figs. 13 and 14)

(between 17 and 14 Ma; Bosworth et al. 2005; Nuriel et al. 2017). In addition, geological fieldwork conducted during three successive research expeditions along the Saudi Arabian margin by the authors (in 2015–2016) shows that the recent pole of opening of the Red Sea has remained invariant at least since the late Oligocene (~27 Ma).

The observed stability of the stage pole of rifting during the late Oligocene to recent time interval allowed us to determine the total angle of rotation Ω through balancing of 23 crustal cross-sections across the Red Sea using the method illustrated in Schettino and Turco (2006) and Schettino (2014). In this approach, crustal profiles are generated and restored palinspastically to the pre-rift configuration. The trace of these profiles is chosen to coincide with flow lines of relative motion about the stage pole, while the profiles are built combining Moho and topography at each

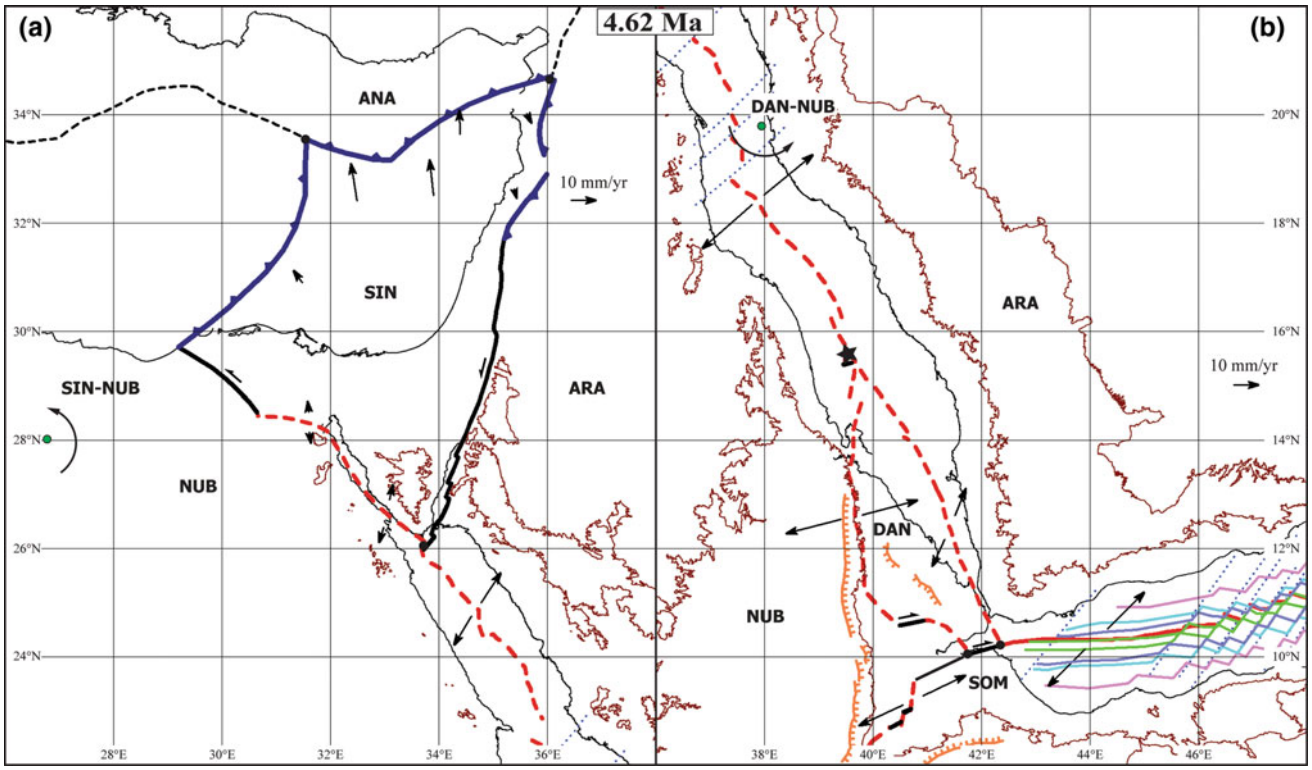

Fig. 3 Plate reconstructions at chron C3n.2ry (4.62 Ma) for the northern Red Sea and eastern Mediterranean (**a**) and for the southern Red Sea, Afar, and western Gulf of Aden (**b**), showing past plate boundaries and velocity vectors of relative motion. Also shown are instantaneous Euler poles of Sinai–Nubia and Danakil–Nubia plate pairs. The star in (**b**) indicates the reconstructed location of the first oceanic crust formed in the southern Red Sea, which coincides with the Danakil–Nubia–Arabia triple junction. Black dots are triple junctions. Red solid lines: Mid–ocean ridges; Red dashed lines: Rift axes; Black dotted lines: Fracture zones and transform faults; Black solid lines: Strike–slip faults; Blue lines with triangular barbs: Convergent boundaries; Orange lines with squared barbs: Major rift structures; Brown lines: Reconstructed modern 1000 m topographic contour. After Schettino et al. (2016)

location along the traces. This method is based on two simplifying assumptions: (1) Crustal mass is conserved along cross-sections during rifting (no transversal flow), and (2) Sediment flow is intra-basinal. The first assumption implies that for any point in the rift valley the ductile flow in the middle–lower crust does not have a component orthogonal to the local velocity vector of relative motion, while the second assumption guarantees that all the balanced mass was originally in the rift region. In addition, the method requires preliminary removal of the oceanic crust in the case of profiles that cross the area of active sea floor spreading. Computation of the pre-rift size of the continental margins at some distance ζ from the Euler pole, $L_0(\zeta)$, and the average stretching factor, β(ζ), requires first the determination of the stretched thickness function $H = H(x,\zeta)$ along the corresponding crustal cross-section, x being the distance along profile, and the initial unstretched crustal thickness $H_0(\zeta)$. Then, if $L(\zeta)$ is the present day size of the rift valley at distance ζ from the Euler pole, the pre-rift restored size, L_0, and the stretching factor, β, will be given by:

$$L_0(\zeta) = \frac{1}{H_0(\zeta)} \int_0^{L(\zeta)} H(x,\zeta)dx \quad (1)$$

$$\beta(\zeta) = L(\zeta)/L_0(\zeta) = \frac{L(\zeta)H_0(\zeta)}{\int_0^{L(\zeta)} H(x,\zeta)dx} \quad (2)$$

In order to determine the function $H(x,\zeta)$ and the quantity $H_0(\zeta)$ for each profile, we compiled a Moho grid for the Red Sea region starting from published data. This is illustrated in Fig. 4 and includes data from several sources (Salem et al. 2013; Hansen et al. 2007; Al–Damegh et al. 2005), as well as oceanic Moho data determined on the basis of the isochron maps of Schettino et al. (2016) and Fournier et al. (2010), respectively for the Red Sea and the Gulf of Aden. To generate the crustal profiles, we combined Moho profiles along the selected traces with Aster GDEM topography. As illustrated in Fig. 5, a total of 23 crustal profiles were created along the central and northern Red Sea, with the objective of

determining the variability of the stretching factor β in the region of separation between Nubia and Arabia and the corresponding finite strain ε. This quantity can be used in turn to estimate the total angle of rotation between Nubia and Arabia, Ω, which restores the pre-rift configuration of the conjugate margins. A plot of the stretching factor, β, as a function of the distance ζ from the Euler pole is shown in Fig. 6, while the corresponding finite strains are listed in Table 1. In this table, the present-day width $L(\zeta)$ at distance ζ from the Euler pole was estimated on the basis of the function $H(x,\zeta)$, which stabilizes to a value $H_0(\zeta)$ at some distance from the rift axis. We note that both β and ε are essentially independent from ζ, despite that we could expect that both rise for increasing ζ, because the relative plate velocity increases with the distance from the Euler pole. However, numerical modelling shows that rifting velocity exerts a control on the strain localization width, so that wide basins have the tendency to form under conditions of slow extension and vice versa (Van Wijk and Cloetingh 2002; Salerno et al. 2016). Therefore, although the rifting velocity $v(\zeta)$ decreases when we move toward the Euler pole, both the initial and present widths of the rift increase, and their ratio remains approximately invariant with respect to ζ. Consequently, by Eq. (2) the quantity β does not change significantly. The average stretching factor resulting from the data listed in Table 1 is: $\beta = 1.47 \pm 0.02$. The corresponding finite strain is: $\varepsilon = \ln(\beta) = 0.39 \pm 0.02$. To assess the sensitivity of these values to errors in crustal thickness H or rift width L, we note that by Eqs. (1) and (2) a very large 10% error in either H or L translates directly into a 10% error in β.

The stretching parameters obtained above can be used to achieve a preliminary estimate of the total angle of rotation that restores the pre-rift configuration. This turned out to be $\Omega = 14.31°$. However, it would not be correct to use this result in a kinematic model of the Red Sea rifting, because there is strong field evidence that a short initial phase of extension occurred during the Oligocene, possibly between 30 and 27 Ma, characterized by N–S extension (i.e., N–S trending strike-slip faults and E–W normal faults) as initially suggested by Makris and Rihm (1991) and Ghebreab (1998). Such an early phase of N–S extension led to the formation of left-lateral pull-apart basins along the rifted margins of Arabia and Nubia. Therefore, a small fraction of the total extension that can be estimated through crustal balancing is not associated with the late Oligocene to recent phase of NE–SW extension but it is related to an earlier stage of separation between Arabia and Nubia. On the basis of kinematic considerations, we suggest that a better estimate for the total angle of rotation during the NE–SW phase of extension is $\Omega = 12.15°$. In this instance, the average angular velocity of separation during the last rifting phase turns out to be $\omega = \Omega/27 = 0.45°$/Myr. The reduced rotation angle $\Omega = 12.15°$ is the angle that brings the N–S trending Great Yemeni Escarpment 1000 m contour to match the corresponding contour line along the Afar Escarpment (see Fig. 8), while more to the north this rotation still shows a gap between the NW–SE oriented 1000 m contour lines of Nubia and Arabia. This observation suggests that an early N–S phase of extension is associated with the residual stretching.

The estimated angular velocity during the NE–SW phase of extension allows us to determine the relative positions of Arabia and Nubia at any time during the late Oligocene—early Pliocene interval, because a unique stage pole characterized this tectonic phase. Similarly, the relative positions of Danakil and Arabia during rifting in the southern Red Sea were determined considering that there is no evidence of changes in the Euler pole of separation between these plates and assuming a constant angular velocity. Finally, the motion of the Sinai microplate with respect to Arabia was determined by extrapolation of the current stage pole and angular velocity (see Schettino et al. 2016). An interesting consequence of this approach is that at 14 Ma (late Langhian) the Danakil microplate displays a tight fit against Nubia, determining complete closure of the Afar Depression (Fig. 7). We interpret this feature as evidence that this microplate started separating from Nubia during the late Langhian, whereby it must be considered as part of Nubia for times older than ~14 Ma. It is also interesting to note that at the same time the western coastline and the southern tip of the Sinai microplate are perfectly aligned with the Arabian Peninsula coastline (Fig. 7). This feature and other geological evidence discussed by Bosworth et al. (2005) support the assumption that the starting time of left-lateral strike-slip motion along the DSFZ is 14 Ma, thereby coinciding with the time of initiation of the main phase of rifting in Afar but more probably related to the time of final collision between Arabia and Eurasia along the Zagros Mountains (Agard et al. 2005; Mouthereau et al. 2007). Although very recent data provide evidence that the formation of the DSFZ occurred earlier by northward propagation in the time interval between 21 and 17 Ma (Nuriel et al. 2017), it is likely that the development of a true plate boundary linked to the global kinematic circuit required more time, therefore we prefer to retain 14 Ma as the representative age of formation of the DSFZ as a plate boundary. We also note that according to Bosworth et al. (2005) extension and rifting initiated in Afar at ~25 Ma. Therefore, our result is much more compatible with geological studies that argue a later time of rifting between Danakil and Nubia and an early rift in the southern Red Sea (e.g., Wolfenden et al. 2004).

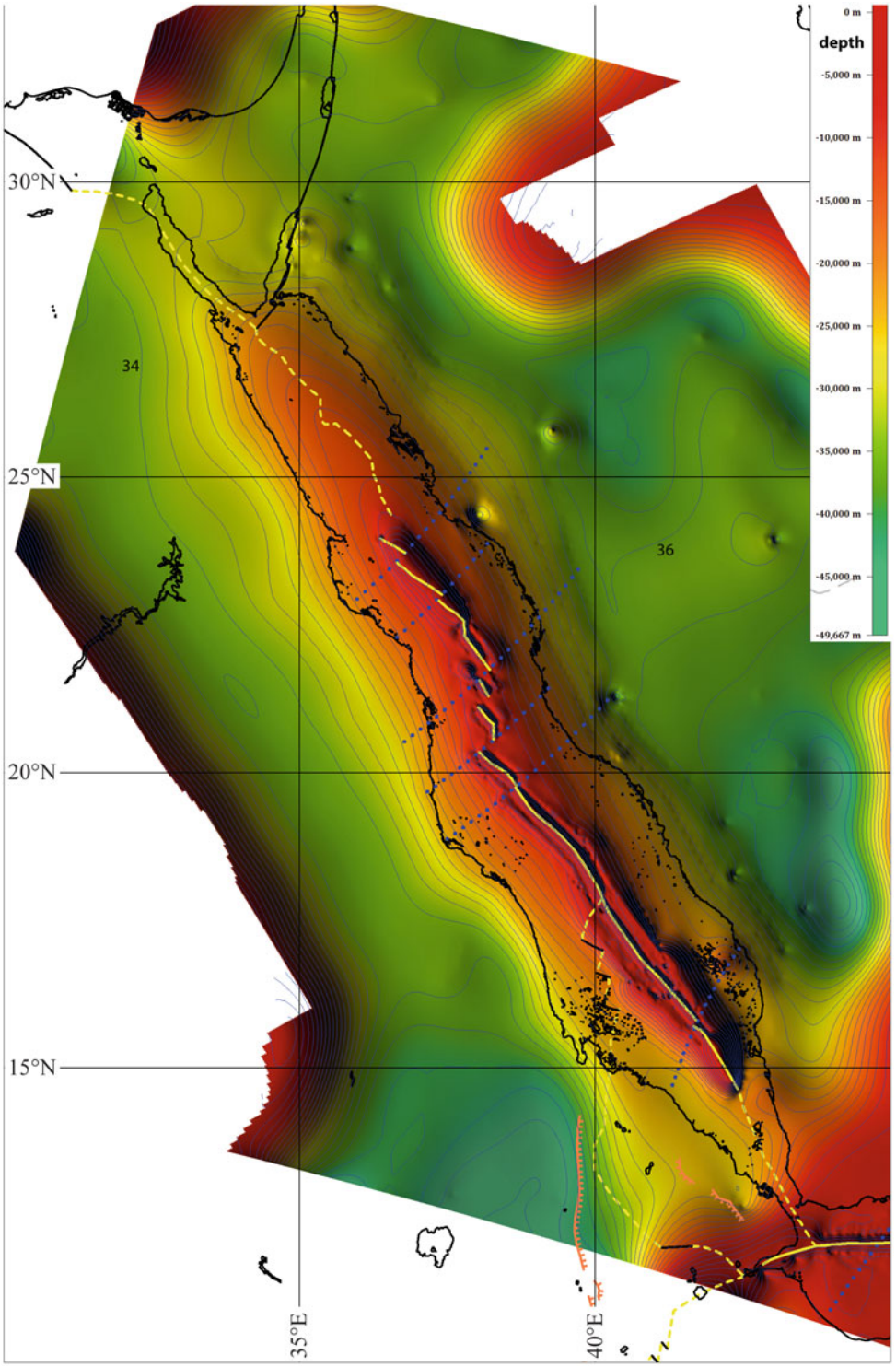

Fig. 4 A Moho map for the Red Sea region. Contour lines are spaced 2 km. Numbers are depths in km

A late Langhian reconstruction of the plate boundaries around the Red Sea is illustrated in Fig. 7 in a fixed Nubian frame of reference. This reconstruction is representative of the time of initiation of rifting between Danakil and Nubia and shows a tight fit of Danakil against the main Afar Escarpment (1000 m contour). Although an earlier phase of extension in Afar is not excluded, it strongly supports kinematic models in which most of the deformation is concentrated in the area to the east of Danakil in the time interval between the late Oligocene and the middle Miocene. Consequently, our preferred scenario assumes that separation of Danakil from Arabia in the southern Red Sea and

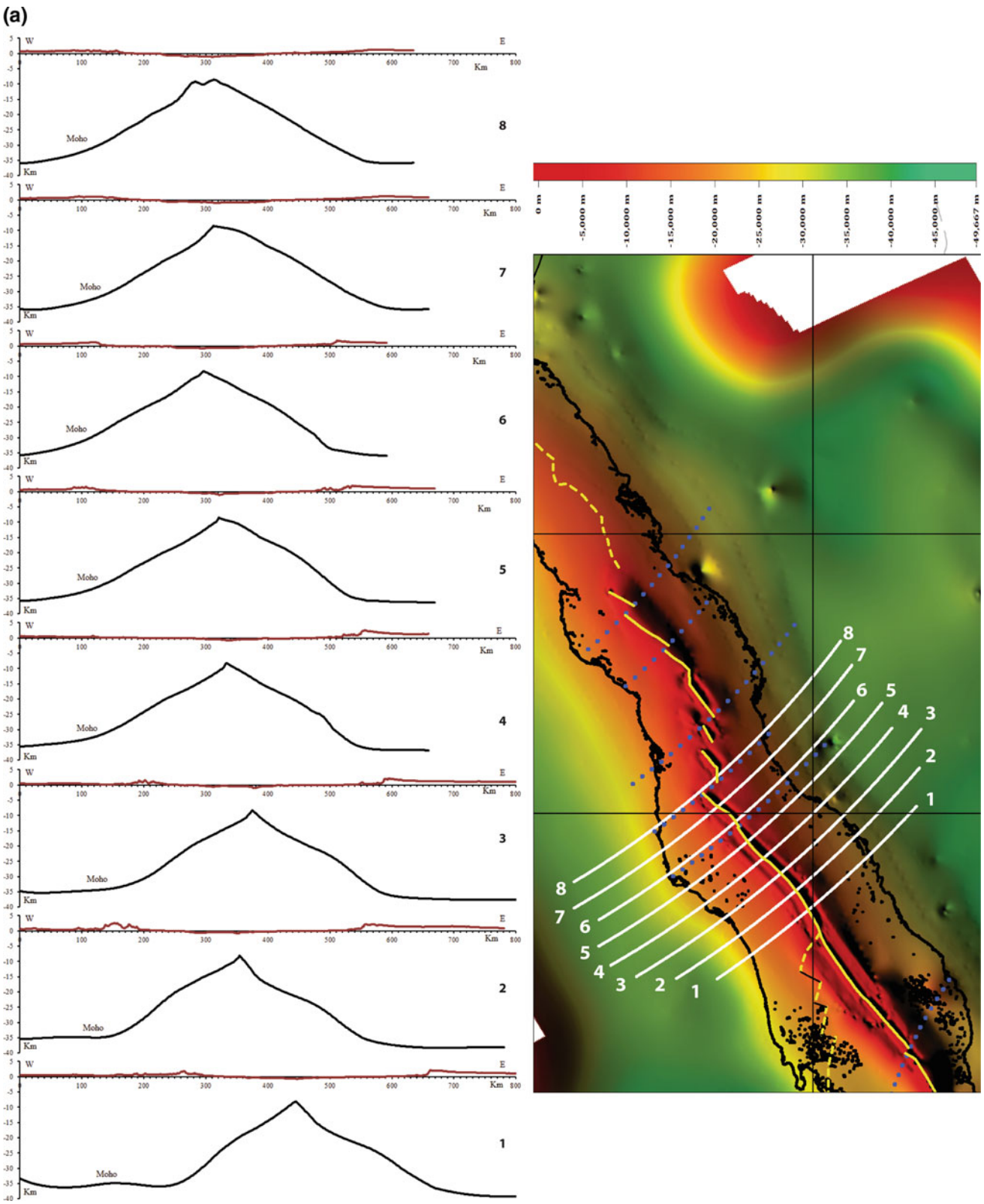

Fig. 5 Crustal profiles across the Red Sea and conjugate thinned continental margins, with the central stripe of oceanic crust. The profiles show the lateral extent of the rift area and follow the flow lines of relative motion between Nubia and Arabia. The map to the right shows Moho depths (see Fig. 4)

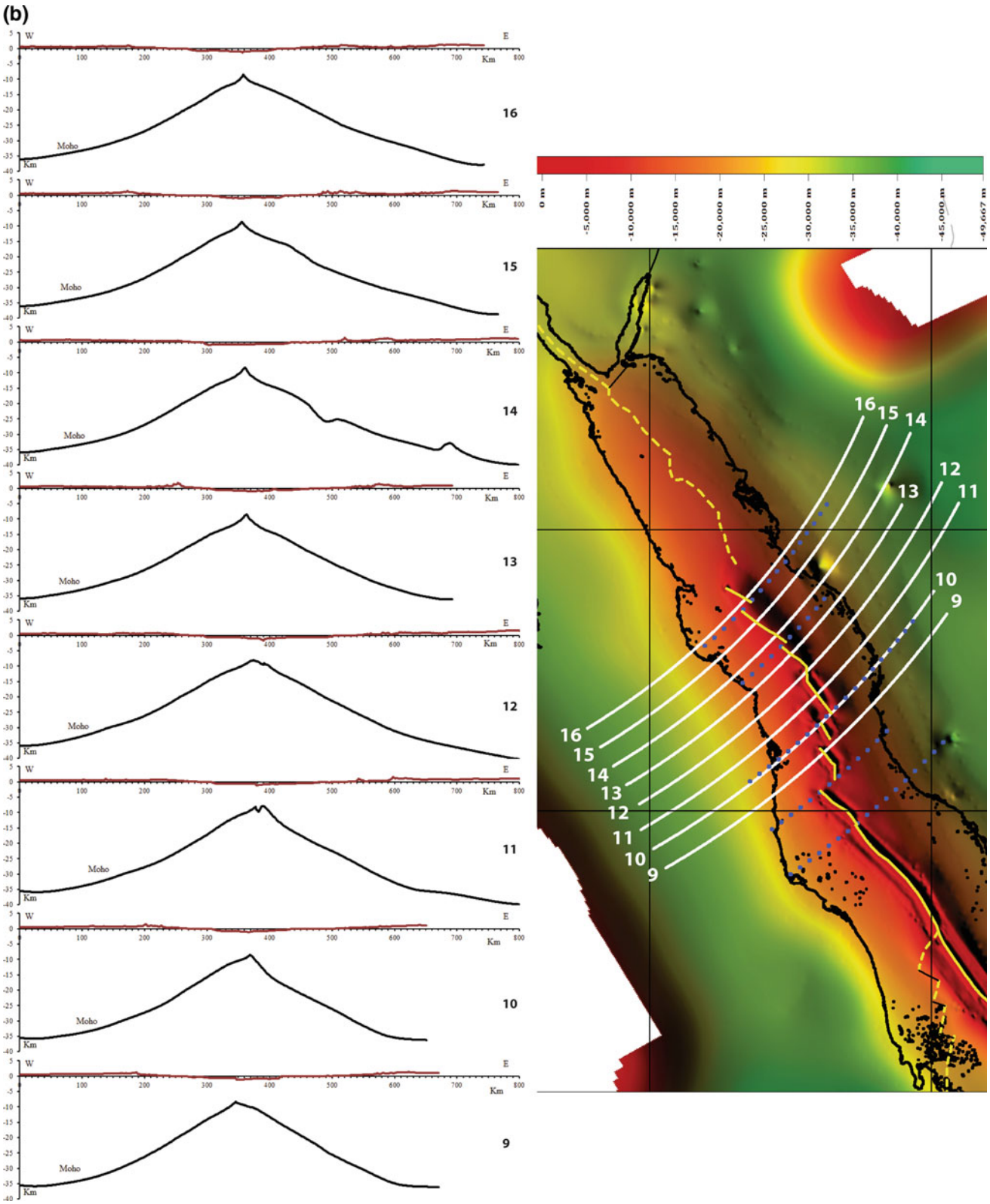

Fig. 5 (continued)

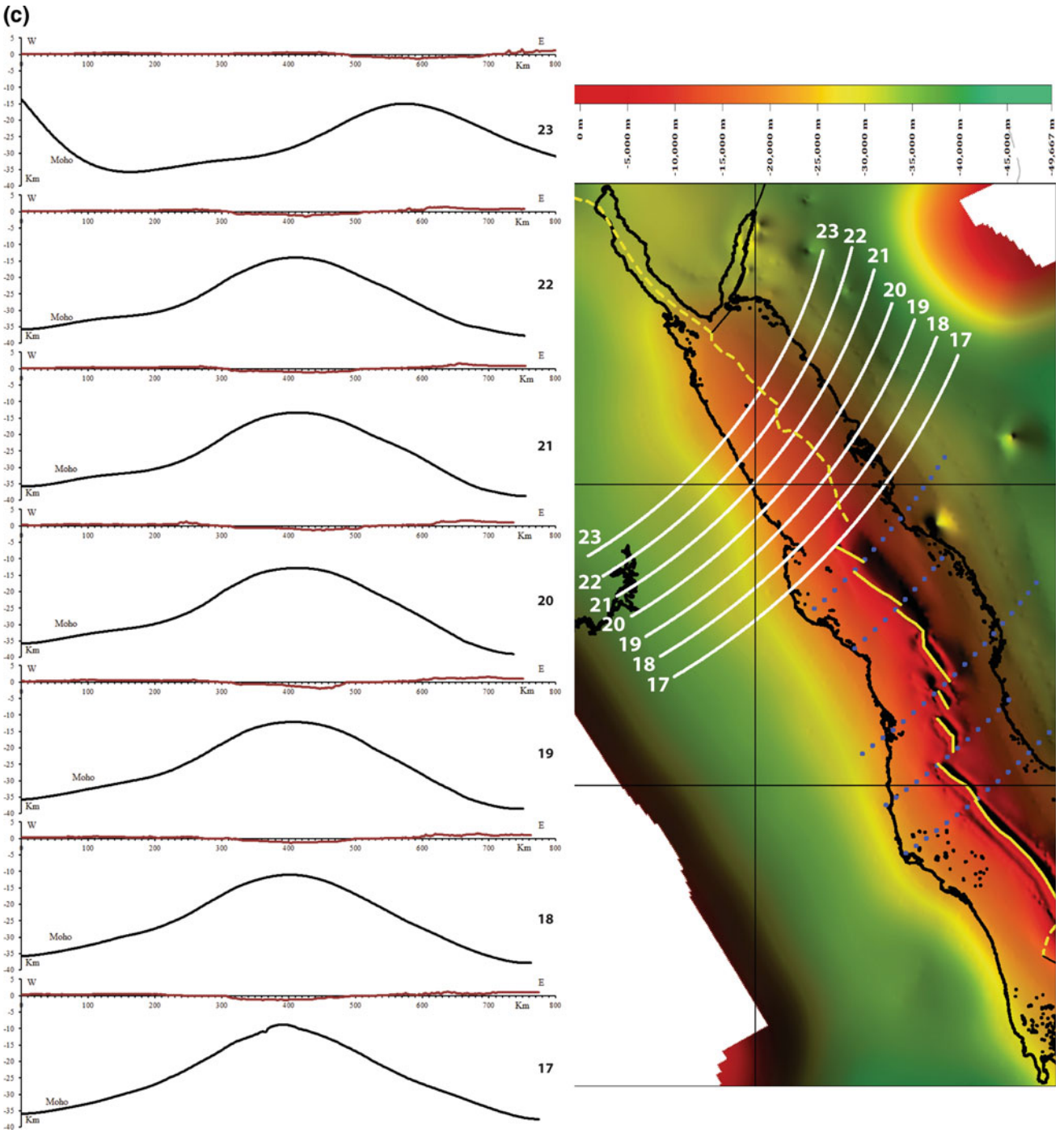

Fig. 5 (continued)

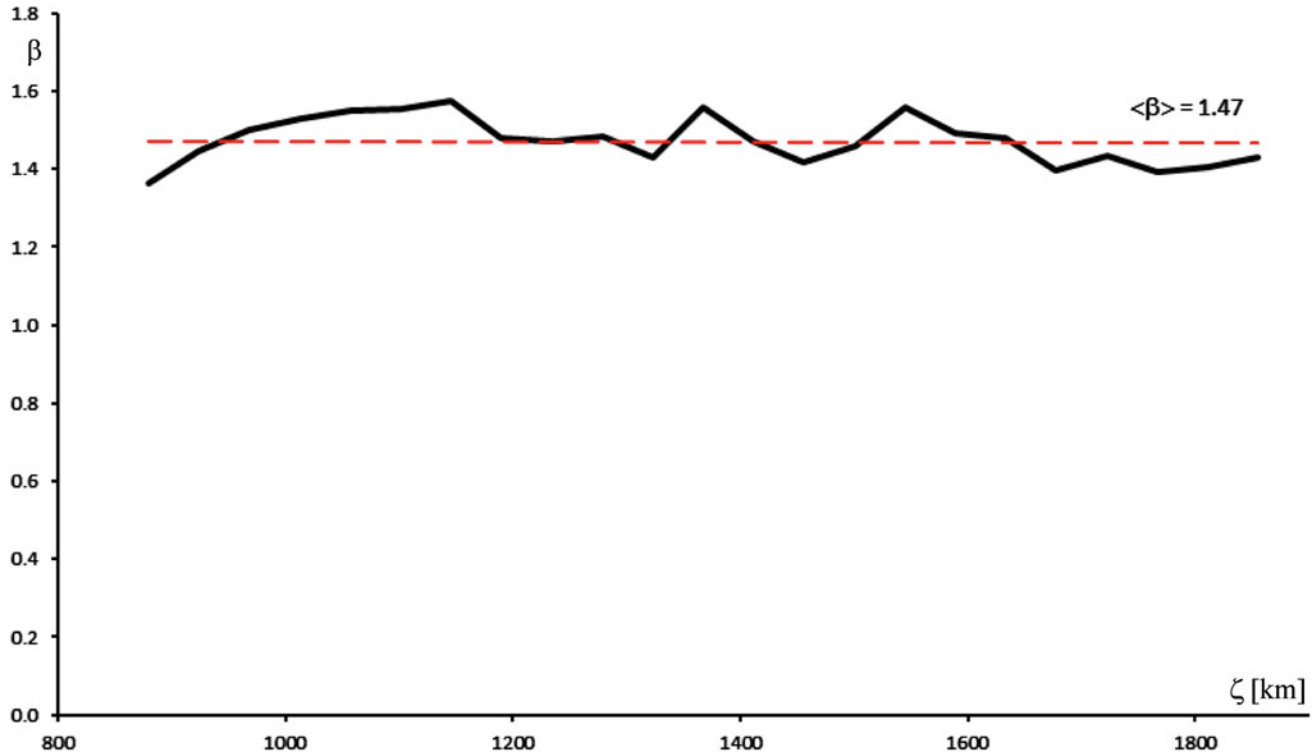

Fig. 6 Estimated beta factor, β, as a function of the distance ζ from the Euler pole of opening of the Red Sea

rifting between Nubia and Arabia in the central and northern Red Sea started simultaneously in the late Oligocene, while partial westward transfer of extension from the southern Red Sea to Afar occurred at a later time during the middle Miocene.

4 Rifting Kinematics During the Late Oligocene—Middle Miocene

The arguments discussed in the previous section imply that Danakil and Sinai were part of the Nubian and Arabian plates, respectively, before the middle Miocene. Consequently, in order to obtain the late Oligocene (27 Ma) configuration, we must keep the Danakil microplate fixed to Nubia and the Sinai microplate attached to Arabia as in the 14 Ma reconstruction. The position of Arabia with respect to Nubia can be obtained applying a clockwise rotation of $\Omega = 12.15°$ from its present-day position about the stage pole of Nubia–Arabia rifting, which is located at 30.32°N, 27.18°E (Schettino et al. 2016). More problematic is determining the relative position of Nubia and Somalia, because a large amount of uncertainty exists about timing and kinematics of rifting events along the East African Rift (EAR). In a recent paper, Fournier et al. (2010) have shown that the oldest pair of magnetic anomalies in the Gulf of Aden has age C6no (20.13 Ma in the geomagnetic polarity time scale of Cande and Kent 1995). Some authors argue that the oldest time of extensional processes along the Main Ethiopian Rift is younger than 11 Ma (e.g., Wolfenden et al. 2004). In this instance, the existence of a precise independent determination of the relative motion between Somalia and Arabia through marine magnetic anomalies would force plate motions in the Red Sea to coincide with plate motions in the Gulf of Aden for times older than 11 Ma, because Nubia and Somalia would form a unique African plate before this time. However, it can be shown that Euler poles from the Gulf of Aden cannot account for the rifting history of the Red Sea during the time interval between 11 Ma and the late Oligocene. Therefore, the formation of the EAR must be older than 11 Ma. Here we assume that Chron C6n (~20.13 Ma) is the initial time of rifting between Nubia and Somalia. This hypothesis does not contrast with the timing determined by marine magnetic anomalies in the Gulf of Aden and is supported by (U–Th)/He thermochronometry observations (Pik et al. 2008).

Figure 8 illustrates the resulting configuration of the plate boundaries and the reconstructed 1000 m topographic contours at 27 Ma. The latter are particularly interesting. If we move northward starting from the Afar zone, we note that the Arabian and Nubian contours display a perfect match between 10° and 15°N, where they have a straight N–S trend. Further north, the two lines both assume a NW–SE trend, but are now separated by a ~40 km gap in N–S

Table 1 Finite strains across the central and northern Red Sea

N	ζ	λ	L	L_0	β	ε'	ε
1	1855	18.29	704	493	1.4284	0.4284	0.3565
2	1811	18.62	694	493	1.4068	0.4068	0.3413
3	1767	18.92	707	507	1.3943	0.3943	0.3324
4	1722	19.21	658	459	1.4325	0.4325	0.3594
5	1677	19.50	664	475	1.3976	0.3976	0.3347
6	1633	19.86	590	398	1.4811	0.4811	0.3928
7	1589	20.12	609	408	1.4942	0.4942	0.4016
8	1545	20.65	602	386	1.5588	0.5588	0.4439
9	1501	21.06	635	436	1.4572	0.4572	0.3765
10	1456	21.57	626	442	1.4162	0.4162	0.3480
11	1412	22.08	795	541	1.4700	0.4700	0.3853
12	1367	22.50	811	520	1.5589	0.5589	0.4440
13	1323	22.78	678	474	1.4291	0.4291	0.3571
14	1279	23.13	795	536	1.4838	0.4838	0.3946
15	1235	23.35	760	516	1.4721	0.4721	0.3867
16	1190	23.76	735	497	1.4787	0.4787	0.3912
17	1145	23.99	772	490	1.5756	0.5756	0.4547
18	1102	24.69	753	484	1.5561	0.5561	0.4422
19	1057	25.20	746	481	1.5521	0.5521	0.4396
20	1013	25.58	736	481	1.5287	0.5287	0.4244
21	968	25.86	750	500	1.5009	0.5009	0.4061
22	924	26.17	751	520	1.4446	0.4446	0.3678
23	880	26.58	804	589	1.3648	0.3648	0.3110

N = Profile number
ζ = Distance from the Euler pole [km]
λ = Latitude of Red Sea axis intersection
β = β factor
L = Rift width [km]
L_0 = Initial width of the rifting area
ε' = Observed engineering strain (= $\beta - 1$)
ε = Observed true strain (= $\ln(1 + \varepsilon')$)

direction up to 15.8°N. This is indicative of an early phase of N–S extension, which could have led to the formation of left-lateral pull-apart basins as suggested by Makris and Rihm (1991) and Ghebreab (1998). Field evidence along the Arabian margin also supports this scenario. Starting from the configuration illustrated in Fig. 8, we can reconstruct the initial shape of the Ethiopian–Yemeni Plateau at ~30 Ma before the onset of rifting and the subsequent break-up of the Pan-African assembly. To this purpose, it is sufficient to rotate southward the Arabian plate about an equatorial pole by ~40 km, as required by the size of the gap. The resulting reassembly of the Ethiopian–Yemeni Plateau is shown in Fig. 9, while the rotation parameters that reconstruct the tectonic history of the plates surrounding the Red Sea are listed in Table 2.

5 Discussion

The kinematic model (and associated tectonic history) of the Red Sea, illustrated in the previous sections, results from a combination of marine geophysical data acquired in the oceanic areas of the Red Sea and the Gulf of Aden (Schettino et al. 2016; Fournier et al. 2010), geological and geophysical observations from the conjugate margins of Nubia, Arabia and Somalia (e.g., Schettino et al. 2016; d'Acremont et al. 2005; Leroy et al. 2010), and balancing of 23 crustal cross-sections across the Red Sea. With respect to other recent kinematic models (ArRajehi et al. 2010; DeMets and Merkouriev 2016), the scenario illustrated above includes and integrates different sources of data, resulting from both

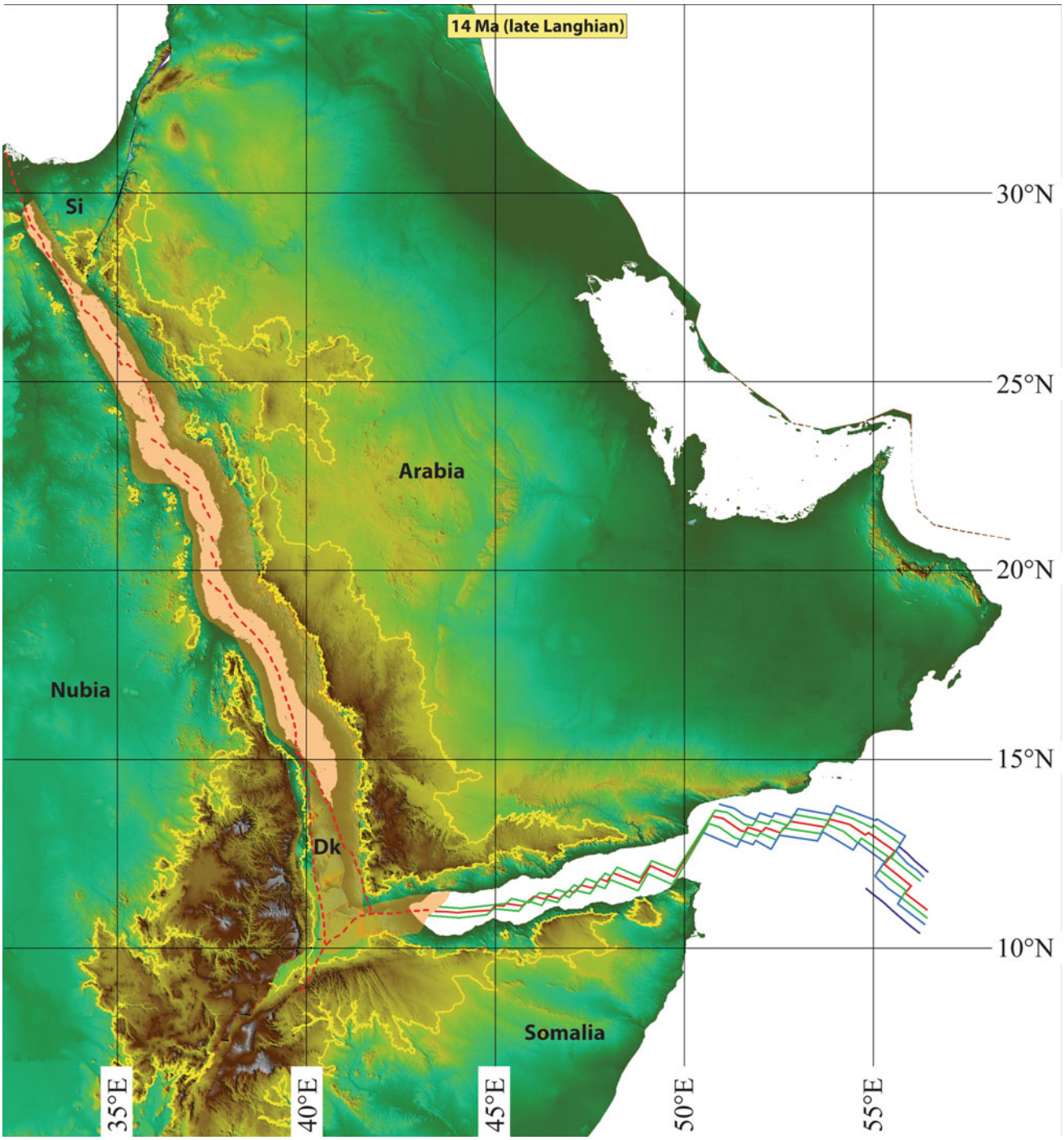

Fig. 7 Reconstruction of the 1000 m topography contour (yellow lines) at 14 Ma (late Langhian) in a fixed Nubian frame of reference. Dk = Danakil microplate; Si = Sinai microplate. The orange area indicates areas of active rifting. Oceanic crust in the Gulf of Aden is indicated by magnetic isochrons 5C (green lines, 16 Ma) and 5D (blue lines, 17.5 Ma) (after Fournier et al. 2010) and by the active spreading ridge (red line)

geophysical and geological observations. A key point in our approach was the determination of the closure angle associated with the pre-rift configuration starting from a palinspastic restoration of the initial size of the rift valley. Although this procedure provided a closure angle $\Omega = 14.31°$, using this parameter would have caused a relevant overlap of the N–S trending 1000 m contour lines of the Great Yemeni Escarpment against the Afar Escarpment. Therefore, we assumed that a small fraction of the total stretching occurred during an early short phase of N–S

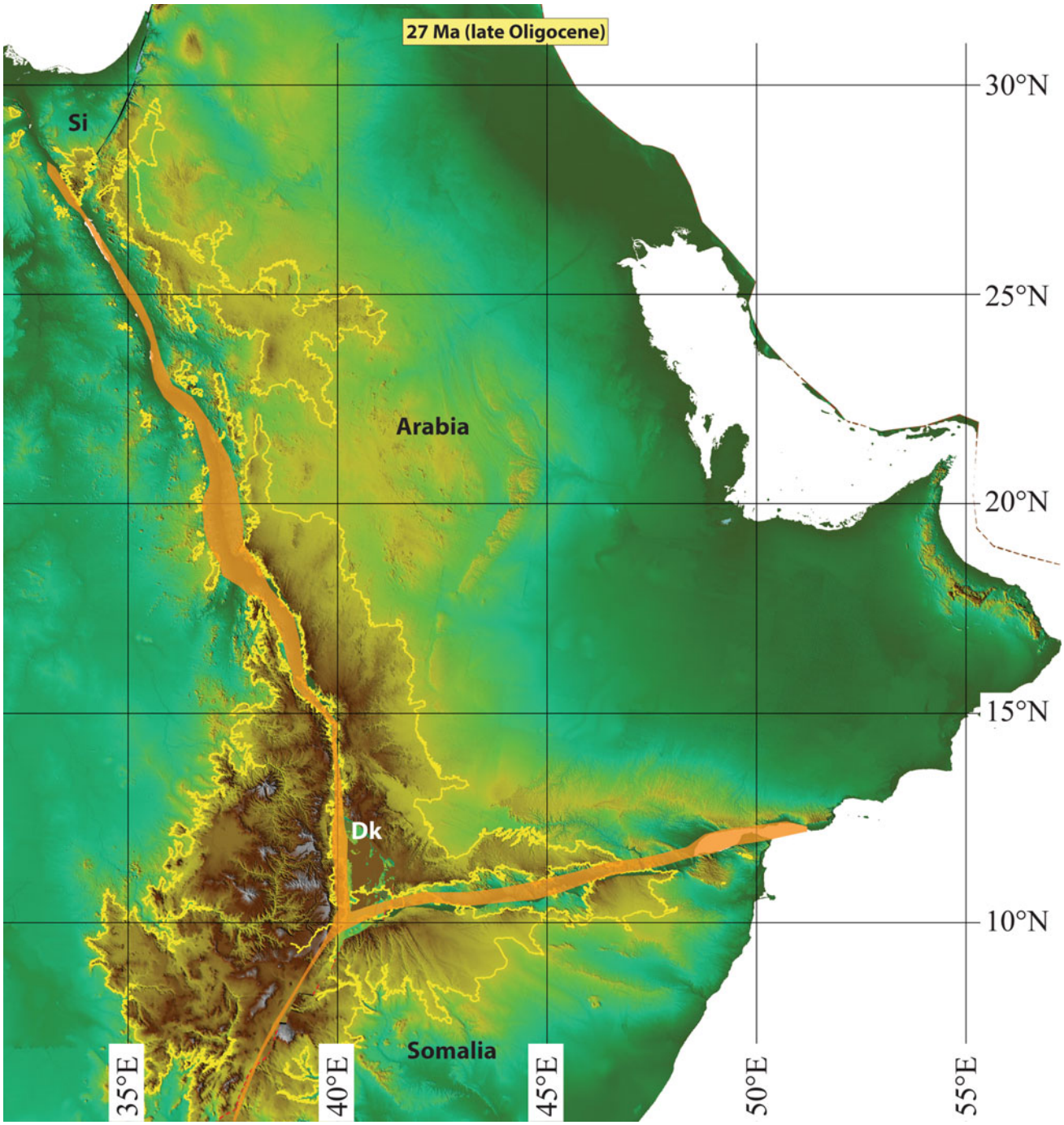

Fig. 8 Reconstruction of the 1000 m topography contour (yellow lines) at 27 Ma (late Oligocene) in a fixed Nubian frame of reference. Dk = Danakil microplate; Si = Sinai microplate. The orange zone indicates areas of active rifting

extension, characterized by the formation of pull-apart basins between Nubia and Arabia, as originally suggested by Makris and Rihm (1991) and Ghebreab (1998). Geological fieldwork conducted during three successive research expeditions along the Saudi Arabian margin by the authors (in 2015–2016) also supports this interpretation. It could be argued that ~40 km of N–S misfit are probably below the resolution of plate kinematics. However, the possibility that the initial stage of formation of the Red Sea was accommodated by N–S strike-slip faults and pull-apart basins does not contrast with some fundamental geodynamic considerations. In fact, the far-field system of forces that drove the

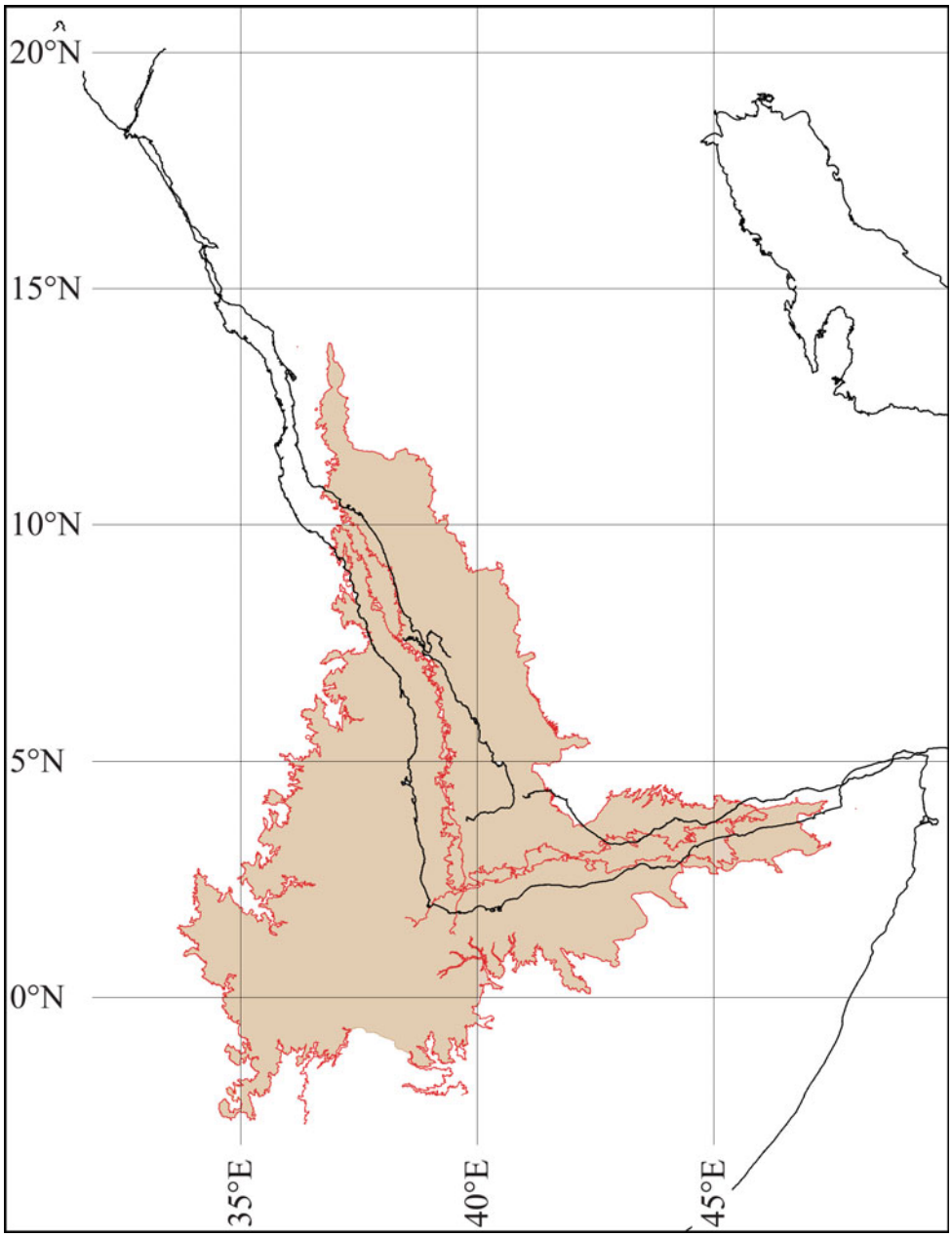

Fig. 9 Reconstruction of the Ethiopian–Yemeni Plateau at ~30 Ma in the palaeomagnetic reference frame of Schettino and Scotese (2005)

initial rifting and rupture between Arabia and Nubia was most probably associated with NE–SW directed slab pull exerted by subducting Neo–Tethys attached to the north-eastern margin of Arabia (Schettino and Turco 2011). In this case, the formation of N–S structures that accommodated the initial phase of extension is perfectly compatible with the orientation of the stress field at that time.

The reconstructions presented in this paper are incompatible with tectonic scenarios that envisage a Red Sea floored entirely or for most of its extent by oceanic crust (e.g., McKenzie et al. 1970; Sultan et al. 1992, 1993). In fact, our starting point was the kinematic model of Schettino et al. (2016) and their isochron map of the Red Sea, which puts a strong constraint on the distribution of oceanic crust in this region. Our reconstructions show that the opening history of the Red Sea can be described by the relative motion of two large plates, Nubia and Arabia, and two intervening microplates, Sinai and Danakil, which formed some time during the Langhian respectively at the northern and southern ends of the rift valley. In the case of Sinai, it was part of the NE-moving Arabian plate from the late Oligocene to the Langhian (~14–16 Ma), in which during this time interval the Red Sea rift continued northward determining the formation of the Gulf of Suez. The details of this process are described extensively in Bosworth et al. (2005). Starting from the Langhian, the onset of left-lateral strike slip along

Table 2 Finite reconstruction poles for the Red Sea and Gulf of Aden regions

Age	Lat	Lon	Angle	References
Arabia–Nubia				
1.77	+30.32	27.18	–0.86	Schettino et al. (2016)
2.58	+30.32	27.18	–1.59	Schettino et al. (2016)
4.62	+30.32	27.18	–3.43	Schettino et al. (2016)
27.00	+30.32	27.18	–12.15	This paper
30.00	+29.87	25.13	–12.25	This paper
Danaki–Arabia				
1.77	+11.68	49.74	–1.26	Schettino et al. (2016)
2.58	+11.68	49.74	–2.00	Schettino et al. (2016)
4.18	+11.68	49.74	–3.38	Schettino et al. (2016)
4.62	+11.68	49.74	–3.76	Schettino et al. (2016)
14.00	+11.68	49.74	–11.86	This paper
Danakil–Nubia				
14.00	–18.14	221.24	+18.42	This paper
Somalia–Arabia				
1.00	+23.67	22.21	+0.52	Schettino et al. (2016)
2.58	+23.67	22.21	+0.94	Fournier et al. (2010)
3.58	+21.28	28.50	+1.62	Fournier et al. (2010)
5.89	+25.46	25.41	+2.40	Fournier et al. (2010)
8.70	+22.56	27.71	+3.99	Fournier et al. (2010)
10.95	+23.88	26.66	+4.74	Fournier et al. (2010)
16.01	+25.85	25.40	+6.85	Fournier et al. (2010)
17.62	+26.10	22.98	+7.28	Fournier et al. (2010)
20.13	+26.46	21.66	+7.83	Fournier et al. (2010)
Somalia–Nubia				
20.13	–41.18	237.32	+1.89	This paper
Sinai–Arabia				
4.62	32.37	27.02	1.28	Schettino et al. (2016)
14.00	32.37	27.02	3.92	This paper

the DSFZ strongly reduced the magnitude of relative motion between Sinai and Nubia and the rift rates in the Gulf of Suez, while the Gulf of Aqaba formed as a pull-apart basin during the development of the DSFZ. Plate kinematics around Danakil is a little bit more complex, because this microplate formed by strain partitioning during the rift between Nubia and Arabia. In the time interval between the late Oligocene and the Langhian (~14 Ma), it was part of the Nubian plate. Consequently, rifting must have started to the east of the Danakil Horst in an ENE direction (~N58–60E, according to the rotation model of Table 2). As mentioned above, such a scenario of late initiation of extension in Afar has been proposed by several authors (Wolfenden et al. 2004; Bonini et al. 2005; Corti 2009) and implies that basaltic magmatism in this area occurred long before a true plate boundary developed between Nubia and Danakil. Starting from the Langhian, the newly formed Danakil microplate moved with respect to both Nubia and Arabia, determining the formation of the Afar Depression. An important feature of the Red Sea rift, which is shared by the Gulf of Aden, is represented by its along-strike segmentation in half-graben sub-basins that are separated by transverse accommodation zones (Bosworth et al. 2005; Leroy et al. 2012). The latter are strongly influenced by pre-existing basement structures, for example by the Najd fault system (Younes and McClay 2002).

A comparison between the relatively complex kinematic model discussed above and more simple plate motion models based exclusively on extrapolation of GPS data can be performed considering the displacement or velocity history of a point along the Nubia–Arabia boundary. This is illustrated in Fig. 10. We note that for a point presently at 9.8°N, 38.6°E both ArRajehi et al. (2010) and Reilinger and McClusky (2011) predict a constant rate between 12 and

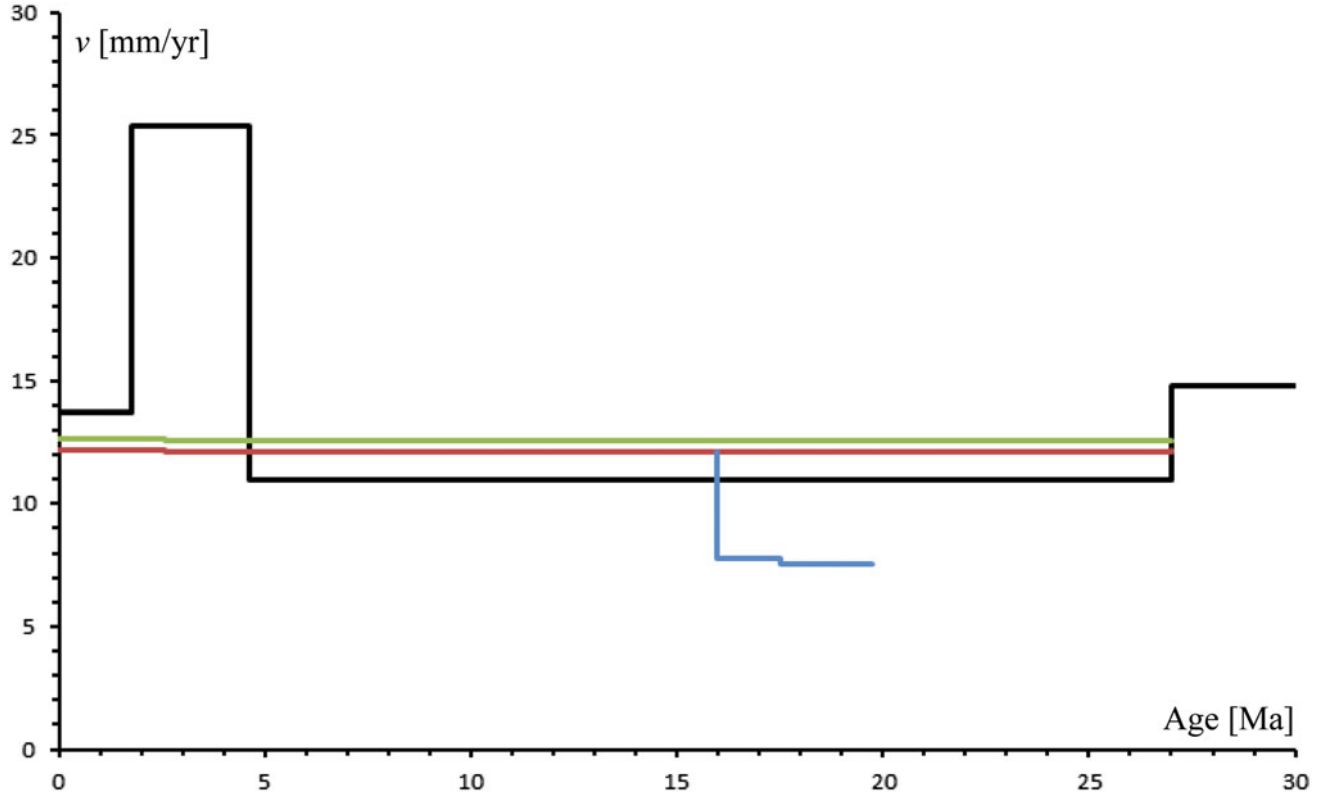

Fig. 10 Predicted spreading/rifting velocities for a point along the Nubia–Arabia boundary, presently located at 19.8°N, 38.6°E. Black line = this paper (and Schettino et al. 2016, in particular the spreading peak between 4.6 and 1.77 Ma); Green line = ArRajehi et al. (2010); Brown line = Reilinger and McClusky (2011); Blue line = DeMets and Merkouriev (2016)

13 mm/yr since the Oligocene, independently from the fact that important geological changes occurred during this long time interval. For example, it is now widely accepted that the rift-drift transition is accompanied by important kinematic changes (Brune et al. 2016). In addition, the end of Neo–Tethys oceanic subduction along the northeastern margin of Arabia (Schettino and Turco 2011) and the subsequent collision with Eurasia, with underthrusting of the Arabian crust beneath Iran starting from ~10 Ma (Mouthereau et al. 2007), cannot be considered uninfluential for plate kinematics. In our model, these two events are associated with an increase of velocity at 4.62 Ma and a subsequent slowdown at 1.77 Ma respectively (Fig. 10). Therefore, the model provides a more realistic view of the tectonic history of the Red Sea region.

6 Conclusion

The kinematic model illustrated above is mainly based on the analysis of marine magnetic data integrated with kinematic indicators observed along the Arabian margin during two research expeditions performed in 2015 and 2016. This model illustrates additional detail on the plate tectonic evolution of the Red Sea since the early Oligocene (~30 Ma). Although a rigorous determination of plate motions in the Red Sea for times older than the late Pliocene is impeded by the absence of magnetic anomalies older than Anomaly 3, structural data show that the Euler poles of relative motion remained stable during most of the rifting stage. Consequently, plate reconstructions of the pre-drift configurations can be obtained by assuming invariant stage poles and performing a palinspastic balance of crustal profiles across the Red Sea. A reconstruction at 27 Ma, which is representative of the onset of NE–SW extension in the Red Sea, supports the idea that a short initial phase of N–S strike-slip between Arabia and Nubia occurred before the development of a system of NW–SE normal faults associated with the main phase of extension.

Acknowledgements This work was funded by the Italian Ministry of University and Scientific Research, PRIN prot. 20125JKANY, and by the Saudi Geological Survey (SGS). The authors are grateful to the SGS personnel who helped them in surveying the area and to the SGS drivers who showed great professionality in their difficult work. Finally, the authors thank four anonymous reviewers for their accurate reviews and useful suggestions that considerably improved this paper.

References

Agard P, Omrani J, Jolivet L, Mouthereau F (2005) Convergence history across Zagros (Iran): constraints from collisional and earlier deformation. Int J Earth Sci 94(3):401–419

Al-Damegh K, Sandvol E, Barazangi M (2005) Crustal structure of the Arabian plate: new constraints from the analysis of teleseismic receiver functions. Earth Planet Sci Lett 231(3):177–196

ArRajehi A, McClusky S, Reilinger R, Daoud M, Alchalbi A, Ergintav S, Gomez F, Sholan J, Bou-Rabee F, Ogubazghi G, Haileab B, Fisseha S, Asfaw L, Mahmoud S, Rayan A, Bendik R, Kogan L (2010) Geodetic constraints on present-day motion of the Arabian Plate: implications for Red Sea and Gulf of Aden rifting. Tectonics 29:TC3011. https://doi.org/10.1029/2009tc002482

Bonini M, Corti G, Innocenti F, Manetti P, Mazzarini F, Abebe T, Pecskay Z (2005) Evolution of the Main Ethiopian Rift in the frame of Afar and Kenya rifts propagation. Tectonics 24(1):TC1007. https://doi.org/10.1029/2004tc001680

Bosworth W, Huchon P, McClay K (2005) The Red Sea and Gulf of Aden basins. J Afr Earth Sci 43(1):334–378

Brune S, Williams SE, Butterworth NP, Müller RD (2016) Abrupt plate accelerations shape rifted continental margins. Nature 536 (7615):201–204

Cande SC, Kent DV (1995) Revised calibration of the geomagnetic polarity timescale for the late Cretaceous and Cenozoic. J Geophys Res 100(B4):6093–6095

Chu D, Gordon G (1998) Current plate motions across the Red Sea. Geophys J Int 135:313–328

Cochran JR (1983) A model for development of Red Sea. Am Assoc Petrol Geol Bull 67(1):41–69

Corti G (2009) Continental rift evolution: from rift initiation to incipient break-up in the Main Ethiopian Rift, East Africa. Earth Sci Rev 96(1):1–53

d'Acremont E, Leroy S, Beslier M-O, Bellahsen N, Fournier M, Robin C, Maia M, Gente P (2005) Structure and evolution of the eastern Gulf of Aden conjugate margins from seismic reflection data. Geophys J Int 160:869–890. https://doi.org/10.1111/j.1365-246X.2005.02524.x

DeMets C, Merkouriev S (2016) High-resolution estimates of Nubia-Somalia plate motion since 20 Ma from reconstructions of the Southwest Indian Ridge, Red Sea and Gulf of Aden. Geophys J Int 207(1):317–332. https://doi.org/10.1093/gji/ggw276

Fournier M, Chamot-Rooke N, Petit C, Huchon P, Al-Kathiri A, Audin L, Beslier M-O, d'Acremont E, Fabbri O, Fleury J-M, Khanbari K, Lepvrier C, Leroy S, Maillot B, Merkouriev S (2010) Arabia-Somalia plate kinematics, evolution of the Aden-Owen-Carlsberg triple junction, and opening of the Gulf of Aden. J Geophys Res 115:B04102. https://doi.org/10.1029/2008JB006257

Ghebreab W (1998) Tectonics of the Red Sea region reassessed. Earth-Sci Rev 45(1):1–44

Hansen SE, Rodgers AJ, Schwartz SY, Al-Amri AM (2007) Imaging ruptured lithosphere beneath the Red Sea and Arabian Peninsula. Earth Planet Sci Lett 259(3):256–265

Joffe S, Garfunkel Z (1987) Plate kinematics of the circum Red Sea—a re-evaluation. Tectonophysics 141(1):5–22

Le Pichon X, Francheteau J (1978) A plate-tectonic analysis of the Red Sea-Gulf of Aden area. Tectonophysics 46:369–406

Le Pichon XT, Gaulier JM (1988) The rotation of Arabia and the Levant fault system. Tectonophysics 153(1):271–294

Leroy S, Lucazeau F, D'Acremont E, Watremez L, Autin J, Rouzo S, Bellahsen N, Tiberi C, Ebinger C, Beslier M-O, Perrot J, Razin P, Rolandone F, Sloan H, Stuart G, Lazki AA, Al-Toubi K, Bache F, Bonneville A, Goutorbe B, Huchon P, Unternehr P, Khanbari K (2010) Contrasted styles of rifting in the eastern Gulf of Aden: a combined wide-angle, multichannel seismic, and heat flow survey. Geochem Geophys Geosys 11(7):Q07004. https://doi.org/10.1029/2009GC002963

Leroy S, Razin P, Autin J, Bache F, d'Acremont E, Watremez L, Robinet J, Baurion C, Denèle Y, Bellahsen N, Lucazeau F, Rolandone F, Rouzo S, Serra Kiel J, Robin C, Guillocheau F, Tiberi C, Basuyau C, Beslier M-O, Ebinger C, Stuart G, Abdulhakim A, Khanbari K, Al Ganad I, de Clarens P, Unternehr P, Al Toubi K, Al Lazki K (2012) From rifting to oceanic spreading in the Gulf of Aden: a synthesis. Arab J Geosci 5:859–901. https://doi.org/10.1007/s12517-011-0475-4

Makris J, Rihm R (1991) Shear-controlled evolution of the Red Sea: pull apart model. Tectonophysics 198(2):441–466

McKenzie DP, Davies D, Molnar P (1970) Plate tectonics of the Red Sea and East Africa. Nature 226(5242):243–248

Mouthereau F, Tensi J, Bellahsen N, Lacombe O, de Boisgrollier T, Kargar S (2007) Tertiary sequence of deformation in a thin-skinned/thick-skinned collision belt: the Zagros Folded Belt (Fars, Iran). Tectonics 26:TC5006. https://doi.org/10.1029/2007tc002098

Nuriel P, Weinberger R, Kylander-Clark ARC, Hacker BR, Craddock JP (2017) The onset of the Dead Sea transform based on calcite age-strain analyses. Geology 45(7):587–590

Pik R, Marty B, Carignan J, Yirgu G, Ayalew T (2008) Timing of East African Rift development in southern Ethiopia: implication for mantle plume activity and evolution of topography. Geology 36(2):167–170

Reilinger R, McClusky S (2011) Nubia-Arabia-Eurasia plate motions and the dynamics of Mediterranean and Middle East tectonics. Geophys J Int 186:971–979

Salem A, Green C, Campbell S, Fairhead JD, Cascone L, Moorhead L (2013) Moho depth and sediment thickness estimation beneath the Red Sea derived from satellite and terrestrial gravity data. Geophysics 78(5):G89–G101

Salerno VM, Capitanio FA, Farrington RJ, Riel N (2016) The role of long-term rifting history on modes of continental lithosphere extension. J Geophys Res 121. https://doi.org/10.1002/2016jb013005

Schettino A (2014) Quantitative plate tectonics. Springer, Berlin, 403 p. ISBN 978-3-319-09134-1

Schettino A, Scotese CR (2005) Apparent polar wander paths for the major continents (200 Ma—present day): a paleomagnetic reference frame for global plate tectonic reconstructions. Geophys J Int 163(2):727–759

Schettino A, Turco E (2006) Plate kinematics of the Western Mediterranean region during the Oligocene and early Miocene. Geophys J Int 166(3):1398–1423

Schettino A, Turco E (2011) Tectonic history of the western Tethys since the late Triassic. Geol Soc Am Bull 123(1/2):89–105

Schettino A, Macchiavelli C, Pierantoni PP, Zanoni D, Rasul N (2016) Recent kinematics of the tectonic plates surrounding the Red Sea and Gulf of Aden. Geophys J Int 207:457–480. https://doi.org/10.1093/gji/ggw280

Sultan M, Becker R, Arvidson RE, Shore P, Stern RJ, El Alfy Z, Guinness EA (1992) Nature of the Red Sea crust: a controversy revisited. Geology 20(7):593–596

Sultan M, Becker R, Arvidson RE, Shore P, Stern RJ, El Alfy Z, Attia RI (1993) New constraints on Red Sea rifting from correlations of Arabian and Nubian Neoproterozoic outcrops. Tectonics 12(6):1303–1319

van Wijk JW, Cloetingh SAPL (2002) Basin migration caused by slow lithospheric extension. Earth Planet Sci Lett 198:275–288

Wolfenden E, Ebinger C, Yirgu G, Deino A, Ayalew D (2004) Evolution of the northern Main Ethiopian rift: birth of a triple junction. Earth Planet Sci Lett 224(1):213–228

Younes AI, McClay KR (2002) Development of accommodation zones in the Gulf of Suez-Red Sea rift, Egypt. Am Assoc Petrol Geol Bull 86:1003–1026